DEVELOPMENT OF TECHNOLOGY FOR PROCESSING UKRAINIAN NICKEL ORES

Tatyana Oliynyk, Liudmyla Skliar

Kryvyi Rih National University, 11 Vitalii Matusevych Str., Kryvyi Rih, 50027, Ukraine
Email: taoliynik@knu.edu.ua, lyuda.cuclina@knu.edu.ua
Corresponding author: taoliynik@knu.edu.uca

ABSTRACT. The study investigates material composition of silicate nickel ores from Zakhidno-Lashchivka area in Ukraine. Mineralogical analysis is carried out on nontronite and ochreous samples. Correlation analysis examines the relationship between mineral composition and the content of Fe, Ni, and Co. Thermodynamic calculations are performed using the ASTRA software package. The optimal parameters for the reduction process in the temperature range of 300–3000 K are determined. Technological studies involve reduction roasting to facilitate leaching of oxidised ore in ammoniac solutions. Magnetic separation of roasted material contributes to the recovery of a non-magnetic product containing 2.5–3.2% Ni and a magnetic fraction with 1.8% Ni. Flotation of the roasted product yields concentrates with 3–5% Ni at a recovery rate of 17-50% (sample 1) and 7.4-46% (sample 2). Magnetic cleaning increases the Ni content in the flotation concentrate to 8% for the nontronite sample (sample 1) and up to 7% for the ochreous sample (sample 2). A process flowsheet is developed, involving roasting at 1000°C for 2 hours, followed by ammoniac leaching. After thickening, precipitation, filtration and drying, nickel product (47% Ni, 0.5% Co, 0.8% Fe) with a moisture content of 65–70% is obtained. Nickel precipitation is performed by heating to 80°C for 1 hour, which allows ammonia to be recycled back into the leaching process.

Keywords: ammoniac leaching, nickel, processing technology, reduction roasting

Introduction

Nickel is currently classified as a critical raw material by both the European Union and the United States (Brown, 2018; Andersson, 2020).

Between 1990 and 2024, a total of 82 large nickel deposits were discovered with combined reserves of 147 million tonnes of nickel. It is important to note that global nickel reserves are distributed highly unevenly. Super-resources are located in Cuba (20 million tonnes) and New Caledonia (20 million tonnes), while large reserves are found in Canada (10 million tonnes) and Indonesia (10 million tonnes). Other resources (46.2%) are spread across 18 countries, each holding between 1 and 10 million tonnes. The nickel content in these deposits also varies significantly. The world's primary nickel resources are found in lateritic weathering crusts (55%), magmatic sulphide ores (28%), and oceanic manganese nodules (17%) (Andersson, 2020; Zhang, 2025).

In China, Canada, and South Africa, sulphide deposits account for 90% to 100% of nickel reserves. In Australia, sulphide ores constitute 50% of the total nickel resources. In contrast, in other countries included in the ranking, nickel extraction predominantly occurs from lateritic deposits. Each year, over 2 million tonnes of nickel are produced globally. Currently, major nickel deposits under development include Weda Bay (Indonesia), Murrin Murrin (Australia), Barro Alto (Brazil), Koniambo (New Caledonia), and Cagdianao (Philippines). Today, nickel production is distributed across various countries, namely: Indonesia – 800000 tonnes per year, Philippines – 420000 tonnes per year, Russia – 270000 tonnes per year, New Caledonia – 220000 tonnes per year, Australia – 180000 tonnes per year, Canada – 175000 tonnes per year, Brazil – 95000 tonnes per year, China – 84000 tonnes per year, Guatemala – 58000 tonnes per year, and Cuba – 52000 tonnes per year. China's nickel production is projected to rise significantly to 1.085 million tonnes by the end of 2025. Meanwhile, forecasts suggest a global nickel deficit could escalate to 839000 tonnes by 2034 – sevenfold the current shortfall (according to the Shanghai Metals Market). The leading nickel producers include Vale (Brazil), Materion (USA), BHP Billiton, South32 (Australia), Anglo American (UK), Glencore (Switzerland), Sumitomo Metal Mining (Japan), and Norilsk Nickel (Russia) (Wani, et al., 2024; Yue, 2024). As of early 2025, the price for nickel (LME Nickel) remains within the range of USD 15360 per tonne (Global nickel mining industry - statistics & facts, https://surl.li/pmfefp).

Major nickel deposits currently under development are silicate ores, with the nickel content of up to 1%, and sulphide ores, containing 1–2% nickel.

According to foreign experts, Ukraine's proven nickel reserves are estimated at 190000 tonnes, accounting for merely 0.4% of global reserves. The country's domestic mineral and raw material base of nickel is represented by exogenous deposits of silicate nickel in weathering crusts. These are concentrated in two regions – the Middle Dnipro area and Middle Pobuzhzhia. The silicate ores of these deposits are of low quality, containing between 0.38% and 1.24% nickel. A total of 12 nickel deposits have been explored in Ukraine, predominantly located in Kirovohrad and Dnipropetrovsk provinces.

In Ukraine, industrial exogenous deposits of nickel and iron-nickel ores are associated with the weathering crust of Precambrian ultramafic rocks. Most of ultrabasic massifs of the Ukrainian Shield (USh) are covered by a lateritic weathering crust of areal type. The thickness of the crust developed on ultramafic rocks generally ranges from 25 to 35 metres, reaching up to 100 metres in certain locations. Three weathering profiles of ultrabasic rocks are identified on the USh: ochre–nontronite, ochreous, and ochre–siliceous. Ochre–nontronite and ochreous profiles are typically formed on gentle uplifts and their slopes.

One nickel deposit (Nove, located in Nikopol area of Dnipropetrovsk region) is associated with the ochreous profile, which contains weakly developed nontronite horizons in some areas. All other known deposits are linked to the ochre-nontronite weathering profile. This typical ochre-nontronite profile is characteristic of ultrabasic rocks of Pobuzhzhia and Devladivka complexes. As a result, Ukraine's nickel ore deposits are concentrated in two regions: Middle Pobuzhzhia

(Pobuzhzhia group of deposits) and the Middle Dnipro area (Devladivka group of deposits).

In addition to the 12 explored deposits, a further 11 minor silicate nickel deposits with cobalt and 48 nickel and cobalt occurrences are identified in Ukraine, although none of these are currently considered to be of industrial significance (Babii et al, 2024).

Thus, Ukraine possesses significant potential for extracting silicate nickel. Nickel deposits may serve as a tool for the green transition, potentially opening doors for co-financing from the EU. Processing silicate nickel ores within Ukraine represents a clear economic opportunity, albeit one currently hindered by substantial technological and financial barriers.

Silicate (oxidised) ores, unlike sulphide nickel ones, exhibit a lower nickel content, a complex mineralogical structure, and significant compositional variations. Consequently, these ores are challenging to process using conventional physical beneficiation methods, necessitating more advanced technological approaches for nickel extraction. This issue is not unique to Ukraine but represents a global challenge in nickel ore processing.

At present, processing silicate (oxidised) nickel ores involves the following methods: ferronickel production, nickel and cobalt production via matte smelting, hydrometallurgical methods, segregation roasting and bioleaching.

Metallurgical processes can generally be categorised into four main types: pyrometallurgy, hydrometallurgy, combined pyro-hydrometallurgical methods, and other specific techniques. Globally, over 20% of nickel is produced using hydrometallurgical technologies, often without prior ore beneficiation.

A critical comparison of the main methods for processing silicate nickel ores, with an emphasis on energy consumption, extraction efficiency, and environmental aspects, is presented in Table 1.

Table 1. *Comparison of silicate ore processing methods*

Method	Energy consumption	Extraction efficiency	Environmental aspects	Comment
Pyrometallurgy	High	Medium	High SO_2, CO_2 emissions, significant amount of slag	Suitable for rich ores; high energy consumption and environmental risks
Hydrometallurgy (HPAL, atmospheric acid leaching)	Medium	High (up to 90-97%)	High wastewater treatment costs, formation of toxic residues	Effective for low-grade ores; complex waste disposal
Biometallurgy (bioleaching)	Low	Potentially high	Minimal emissions, environmentally friendly	Lengthy leaching cycle, difficulty in scaling up

Hydrometallurgical processing is predominantly applied to low-grade limonitic ores and encompasses several advanced techniques, including high-pressure acid leaching (HPAL), atmospheric acid leaching, a combination of both methods, heap leaching and different emerging technologies

Hydrometallurgical processing of nickel-containing raw materials employs either ammoniac or acid leaching techniques. Freeport and Sherritt-Gordon refine the ammonia-carbonate technology, successfully implementing it at Yabulu and Surigao Plants. Hydrometallurgical methods for nickel extraction are also used at Pedro Soto plant (Cuba) and São Paulo plant (Brazil). In recent years, there has been an increasing industrial trend towards applying solvent extraction and sorption processes to nickel production. This approach is implemented at Sumitomo Metal Mining and Nippon Mining Plants in Japan (Andersson, 2020; Pandey, 2023).

A 2022 study suggests a new technology for extracting nickel and cobalt from iron-silicate ores, achieving nickel extraction efficiency of up to 97% and cobalt up to 92.8%. The method involves using calcium hypochlorite and ammonium fluoride in an HCl solution at room temperature, which avoids high energy consumption and simplifies the process (Kenzhegali et al, 2022).

A 2024 technology review highlights that the hydrometallurgical processes face challenges with impurity leaching, complicating nickel and cobalt extraction. Pyrometallurgical methods are associated with high energy consumption and environmental risks. Therefore, future developments in this area should focus on energy conservation and emission reduction (Qinglong et al, 2024).

Traditional pyrometallurgical processes primarily include the ferronickel process and the nickel matte process.

The ferronickel process encompasses smelting in an electric furnace, rotary kiln smelting, and blast furnace smelting.

The nickel matte process involves sulphide smelting in a blast furnace, sulphide smelting in a rotary furnace, sulphide smelting in a ferronickel converter, and sulphide smelting in an oxygen-enriched side-blown furnace (Li, et al., 2015; Tian, 2023).

Both hydrometallurgical and pyrometallurgical processes present notable disadvantages. For instance, hydrometallurgy is associated with high capital costs, significant acid consumption, and complex tailings treatment. Pyrometallurgy, on the other hand, is characterised by high energy consumption, considerable greenhouse gas emissions, and environmental pollution.

To overcome these challenges, a combined metallurgical process has been developed. This innovative hybrid approach incorporates various additives for oxidative or reduction roasting at relatively low temperatures. Its key advantages include modifying the structure, phase composition, and oxidation state of nickel- and iron-containing minerals, such as goethite and serpentine, as well as enhancing solubility of ores and increasing efficiency of valuable metal extraction (Li et al., 2019; Nurjaman, 2020; Zappala, 2023).

In recent years, scholars have developed an increasing number of innovative methods for nickel extraction, with bioleaching and chlorination being particularly noteworthy.

Biological leaching of nickel (biometallurgy) is an environmentally friendly method for extracting metals from ores using microorganisms. This process is actively applied in countries around the world, namely in Australia, Finland, and Indonesia.

Bioleaching utilises microorganisms to extract nickel, offering significant advantages in terms of environmental safety and cost-effectiveness.

Titan Resources (Australia) is notable for developing the BioHeap process, which efficiently leaches nickel from low-grade sulphide ores using thermophilic bacteria. This method eliminates the need for fine ore grinding, reducing costs and enabling processing of ores with a low nickel content (Boroumand, Z., 2025). Terrafame (Finland) utilizes bioleaching for extracting nickel, zinc, and copper from polymetallic ores. According to an independent life cycle analysis, production of 1 kg of nickel sulphate using this technology emits only 32% of the CO_2 compared to traditional methods. This translates to an avoidance of 620000 tonnes of CO_2 emissions annually. In Indonesia, bioleaching of nickel ores using the *Aspergillus niger* fungus is under study**.** This fungus produces citric acid**,** which effectively dissolves nickel from the ore (Roberto, 2022).

Chlorination involves converting useful metals in ores into chlorides by using specific agents, enabling their subsequent extraction. This method is distinguished by its adaptability, short technological cycle, and high degree of comprehensive utilisation. However, despite their potential benefits, these emerging technologies have yet to achieve widespread industrial adoption (Chaerun, 2017; Santos, 2020; Chaerun et al., 2023).

Based on the analysis of current nickel ore processing, hydrometallurgy shows promise for treating low-grade silicate ores, though it requires solutions for waste disposal. Pyrometallurgy remains relevant for high-grade ores, but it involves high energy consumption and environmental risks. Biometallurgy holds potential as an environmentally friendly technology, but it needs further research for scaling up.

Ukrainian nickel ores are characterised by their low nickel content and necessitate specific processing technologies that inherently involve advanced beneficiation methods. Based on the current state analysis of oxidised nickel ore processing, the most promising approach for beneficiation is reduction roasting. This method can be combined with subsequent mechanical beneficiation and chemical leaching. Furthermore, reduction roasting can be integrated with processes for extracting pure products from nickel-containing solutions.

The research aim is to develop a beneficiation technology for Ukrainian nickel ores on the basis of a detailed analysis of the chemical composition and technological properties of nontronite samples derived from ultrabasic rocks, which are characterised by a low nickel content in the raw material.

Materials and Methods

Two ore samples from the Zakhidnolashchivska area of silicate nickel ores were submitted for research. This area is located in the central part of the Holovaniskyi block, on the left bank of the Southern Buh River, 5 kilometres southeast of Pobuzhskyi Ferronickel Plant. The chemical composition of the technological samples is provided in Table 2, while their physical properties are detailed in Table 3.

The physical properties of the nontronite and ocherous samples, including density, specific surface area, and inclination angle, exhibit no significant differences.

The granulometric analysis of the ore, ground to a particle size of 2 mm, is presented in Figure 1.

Table 2. *Chemical composition of laboratory-technological samples, %*

№	Fe^0_{tot}	Fe_2O_3	FeO	SiO_2	Al_2O_3	CaO	MgO	TiO_2	MnO	Cr_2O_3	P_2O_5	NiO	Na_2O	K_2O	evaporation loss	CO_2	S
1	16.8	22.3	1.5	48.48	4.81	2.63	6.9	0.35	1.12	0.75	0.05	0.73	0.10	0.29	9.27	0.71	0.01
2	34.4	47.5	1.5	26.9	5.87	0.79	3.07	0.51	0.75	0.99	0.078	0.61	0.058	0.026	11.17	0.16	0.015

Table 3. *Physical properties of laboratory-technological samples*

Raw material	Density kg/m³ × 10^3	Bulk density, kg/m³ × 10^3		The specific surface area, m²/kg	Inclination angle
		With out compaction	With manual compaction		
Sample 1	4.64	1.13	1.42	872.33	37^0
Sample 2	4.67	1.14	1.44	878.38	36^0

The results of the analysis indicate that the mass fractions of nickel and total iron are uniformly distributed across the particle size classes. The sieve characteristics are described by exponential equations:

- $y = 43{,}713e^{-2{,}0471x}$ (Sample 1)
- $y = 66{,}515e^{-1{,}8143x}$ (Sample 2)

The approximation reliability is: $R^2 = 0.979$ for Sample 1, and $R^2 = 0.9237$ for Sample 2.

This indicates (Figure 1) the presence of fine-grained classes in the ore, and that the ores belong to easily ground raw materials.

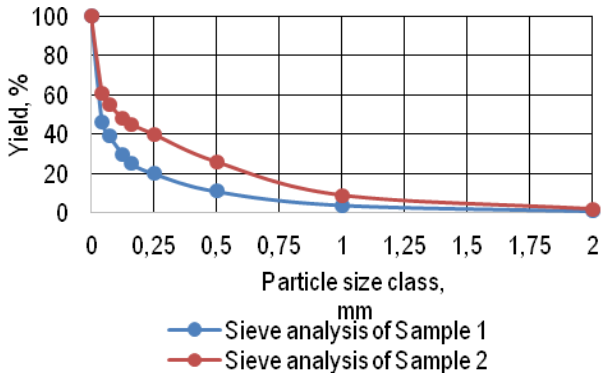


Fig. 1. Sieve analysis of the nickel-bearing ore ground to a particle size of 2–0 mm

Mineralogical composition of ore samples

The mineral composition (in vol. %) of the nontronite-montmorillonite sample (Sample 1) and the ochre-

montmorillonite sample (Sample 2) from the laboratory-technological analysis is provided in Table 4.

Table 4. *Mineral composition (vol.%) of the laboratory-technological samples*

Minerals	Sample 1	Sample 2
Hydrobiotite	5.50	3.32
Hydrogoethite	4.71	73.44
Quartz	10.62	4.43
Beidellite	3.26	0.77
Nontronite	69.17	14.46
Magnetite	0.80	0.79
Maghemite	5.42	1.92
Hematite	0.03	0.27
Chromite	0.44	0.36
Ilmenite	0.04	0.23
Chalcopyrite	0.01	0.01
Total	100.00	100.00

The results of a detailed mineralogical analysis of the samples are presented below.

Nontronite is the principal rock-forming mineral, (over 50.0 vol.% in sample 1) in hydro-micaceous-nontronite, ochre-nontronite, nontronite, as well as gruss-clayey and ochre-clayey varieties of supergene ores. The latter two can be combined with the ochreous-nontronite variety.

Furthermore, nontronite is present in nontronite-montmorillonite and ochreous varieties, with its content ranging from 4.0 to 38.0 vol.%. The mineral is characterised by a brown to greenish-brown colour (Figure 2a, b).

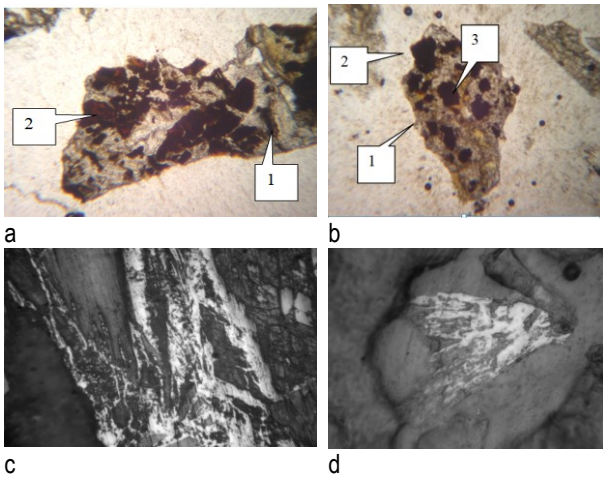


Fig. 2. Sample ore minerals
a, b – replacement of primary silicates with montmorillonite (1), accompanied by the release of excess iron in the form of iron-containing minerals: hydrogoethite (2) and hydrobiotite (3); c – goethite-hydrogoethite aggregate (1) in a hydrobiotite fragment; fraction -2.0+1.0 mm; magnification 80×;d – hydrogoethite radial-fibrous aggregate in a silicate fragment; fraction -0.125+0.074 mm; magnification 200×.

It occurs both as "free" fragments and as aggregates in association with hydrogoethite, hydrobiotite, chlorite, montmorillonite, maghemite, chromite, and ilmenite. These aggregates disintegrate under minimal pressure, resulting in the near-complete (approximately 100%) release of nontronite.

Montmorillonite is a rock-forming mineral found in the majority of nickel-containing rock varieties. It appears as dirty-green to green inclusions (Figure 2a, b) and is observed both as "free" fragments and as aggregates with hydrobiotite, maghemite, chromite, and ilmenite. These aggregates disintegrate under minimal pressure, resulting in the near-complete (approximately 100%) release of montmorillonite.

When exposed to water, montmorillonite exhibits significant swelling, leading to a substantial increase in volume. Following this, it readily disintegrates into fine particles. X-ray diffraction analysis reveals a considerable admixture of saponite within the montmorillonite.

Hydrogoethite and goethite are the principal minerals in the nontronite-ochreous and ochreous varieties of ores. They are also present as secondary minerals in other ore varieties. Hydrogoethite is characterised by a yellowish-brown to reddish hue, while goethite exhibits colours ranging from dark brown to black. These minerals occur as free fragments (Figure 2c,d; Figure 3c) and as aggregates with nontronite, quartz, and black ore minerals, such as maghemite, chromite, and ilmenite. On the surfaces of these minerals, hydrogoethite forms coatings. In aggregates with silicates, hydrogoethite occasionally develops colloform and radial-fibrous structures.

Goethite, meanwhile, appears as sheath-like aggregates within silicate fragments and frequently forms solid spherulites, which are typically rimmed with hydrogoethite.

Quartz is present in varying quantities, ranging from 0.1 to 17.0 vol.%, across nearly all varieties of nickel-containing rocks, excluding the nontronite-montmorillonite variety. The mineral is transparent to translucent. Quartz fragments exhibit angular to slightly rounded shapes, with rounded fragments being relatively uncommon (Figure 3a). Aggregates of quartz with nontronite and ore minerals are occasionally observed, whereas associations with hydrobiotite are rare. In several samples, a cryptocrystalline form of quartz — chalcedony — has been identified. The size of quartz fragments varies from 0.07 to 1.0 mm, with the majority falling within the range of 0.2 to 0.5 mm.

Hydrobiotite is present as a secondary and accessory mineral in all varieties of low-grade nickel ores. The mineral predominantly exhibits a brownish-yellow hue, although flakes in shades of yellow and greenish-yellow are occasionally observed.

Nearly all hydrobiotite fragments are released from other minerals; however, in larger fragments, aggregates of hydrobiotite with nontronite are sometimes present (Figure 4c). The size of the flakes ranges from 0.05 to 1.0 mm, with the majority measuring between 0.1 and 0.2 mm. X-ray diffraction analysis of the samples studied reveals the presence of vermiculite in addition to hydrobiotite. The hydromica fragments exhibit a complex interstratified structure, incorporating elements of both hydrobiotite and vermiculite. The overall trend, demonstrating the predominance of iron over magnesium, further confirms the quantitative dominance of hydrobiotite over vermiculite. Therefore, in this study and subsequent discussions, occurrences of hydromicas will be referred to as hydrobiotite.

Beidellite is recognised as an accessory mineral across all ore varieties. In some instances, its content reaches up to 20.0 vol.%. However, it is generally absent or does not exceed 3.0%. Microscopically, it appears as a typical layered clay mineral of

white or yellowish-white colour. Under minimal pressure, it easily disintegrates into fine particles.

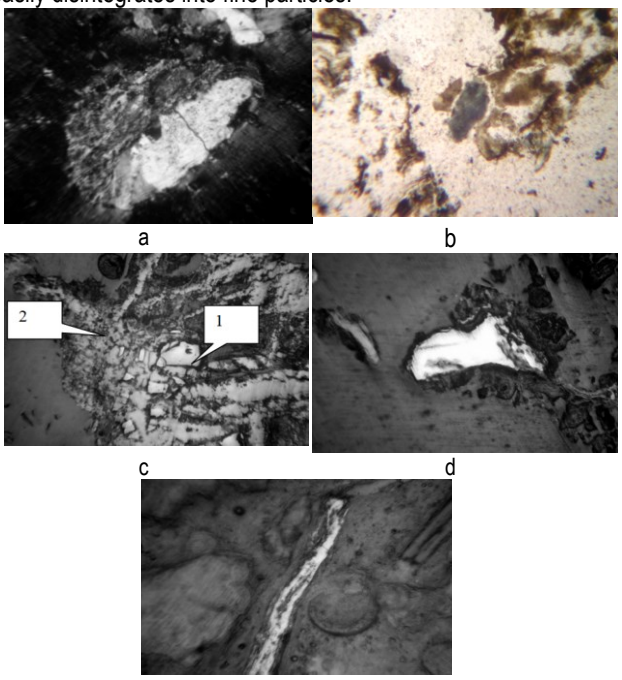


Fig. 3. Sample non-ore minerals
a – quartz occurrences in standard samples; transmitted light; magnification 30×; b – free chlorite fragment (1) among montmorillonite particles (2); magnification 30×; c – hydrogoethite aggregate (2) with a higher concentration of magnetite inclusions (1); particle size class –1.0+0.5 mm; d – free flaky fragment of maghemite; particle size class -2.0 mm; magnification 80×; e – isometric free fragment of chromite; fraction –0.16+0.125 mm; magnification 100×

Beidellite most commonly occurs in aggregates with quartz, less frequently with hydrobiotite, and occasionally with black ore minerals.

Manganite, along with nontronite, is identified as a primary mineral. It appears in the form of brownish-black earthy aggregate lumps. When ground against white porcelain, it produces a chestnut-brown powder. The identification of manganite is verified through spectral analysis.

Serpentine is present in trace quantities, accounting for approximately 1.0 vol.%. It appears as yellowish-green remnants with a poorly defined fibrous texture. The mineral particles contain inclusions of non-magnetic black ore minerals, such as ilmenite and chromite.

Chlorite is observed in certain standard samples from the studied area, with its content ranging from 1.3 to 5.1 vol.%. Its presence is verified through microscopic examination and X-ray diffraction analysis. Chlorite is spatially associated with nontronite, montmorillonite, and hydrobiotite, although isolated fragments are occasionally identified. The predominant flake size of chlorite varies between 0.01 and 0.1 mm.

Magnetite is an accessory mineral found in all varieties of nickel-containing rocks, making it a characteristic feature of both laboratory-technological samples 1 and 2. It occurs as a relict component within goethite-hydrogoethite aggregates, as inclusions in silicate fragments, and as separate free grains in finer fractions (-0.25 mm). The grain size of magnetite ranges from 0.025 to 0.2 mm.

Hematite is spatially and genetically associated with magnetite. It is present within magnetite aggregates as well as in veinlets within silicate fragments, although its overall occurrence is insignificant.

Maghemite is characteristic of both laboratory-technological samples. Morphologically, it occurs as spherulitic clusters, individual spherolites, and flaky fragments. Skeleton-like aggregates are also observed (Figure 3 c,d). The size of maghemite fragments and spherulites ranges from 0.07 to 0.3 mm.

Chromite occurs as fractured, isometric fragments ranging from 0.02 to 0.2 mm in size, within the material of nontronite and ocherous samples (Figure 3e).

Ilmenite is identified as platy individuals in aggregates with silicates such as nontronite, montmorillonite, and hydrobiotite. Free ilmenite fragments are also observed. In polished thin sections, ilmenite appears as elongated plate-like cross-sections (Figure 4a), with elongation sizes ranging from 0.005 to 0.1 mm.

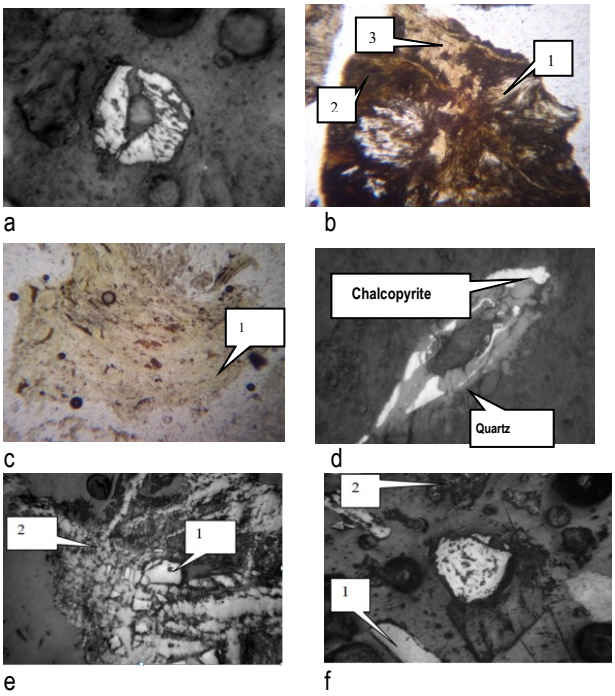


Fig. 4. Sample accessory minerals
a – fragment of a free ilmenite plate (the plate is obliquely inclined to the polished surface of the thin section); fraction – 0.16+0.125 mm; magnification 200×; b – fibrous aggregates of amphibole (1), layered accumulations of nontronite (2), remnants of pyroxene (3); c – hydrobiotite flakes (1) in a nontronite fragment; transmitted light; Nicols; magnification 30×; d – chalcopyrite-quartz fragment; particle size fraction –0.25+0.16 mm; magnification 200×; e – hydrogoethite aggregate (2) with a higher concentration of magnetite inclusions (1); particle size class -1.0+0.5 mm; f – free magnetite fragment (in the centre) among goethite (1) and silicate (2) fragments; particle size class –0.25+0.16 mm.

Chalcopyrite, the rarest mineral in the analysed samples, is present both as free fragments and in aggregates with quartz (Figure 4d). The grain size of chalcopyrite ranges from 0.001 to 0.05 mm.

To examine the relationship between the mineral composition and the Fe_{tot}, Ni, and Co content, a correlation analysis was conducted for laboratory-technological samples 1 and 2. The results for sample 1 are summarised in Table 5 and in Figure 5. A positive correlation was observed between the quantity of black ore minerals and Fe_{tot} ($r = 0.43$). Conversely, a

negative correlation is identified between the content of hydrobiotite and nontronite (r = -0.62), as well as between hydrogoethite and nontronite (r = -0.69). No significant correlations are established among other components in the correlation matrix presented in Table 5.

Table 5. *Correlation matrix of the mineralogical and partial chemical composition of sample 1*

	Ore minerals	Hydrobiotite	Nontronite	Hydrogoethite	Quartz	Kaolinite	Fe_{tot}	Ni	Co
Ore minerals	1.0	-.24	-.00	-.13	-.16	-.26	.43	.15	.25
Hydrobiotite	-.24	1.0	-.62	.20	.06	.05	-.36	-.05	-.22
Nontronite	-.00	-.62	1.0	-.69	-.38	-.38	.01	-.13	.13
Hydrogoethite	-.13	.20	-.69	1.0	.04	-.02	.38	.18	-.08
Quartz	-.16	.06	-.38	.04	1.0	.37	-.30	.00	-.01
Kaolinite	-.26	.05	-.38	-.02	.37	1.0	-.33	-.01	-.13
Fe_{tot}	.43	-.36	.01	.38	-.30	-.33	1.0	.39	.24
Ni	.15	-.05	-.13	.18	.00	-.01	.39	1.0	.00
Co	.25	-.22	.13	-.08	-.01	-.13	.24	.00	1.0

The correlation matrix for sample 1 is plotted in Figure 5.

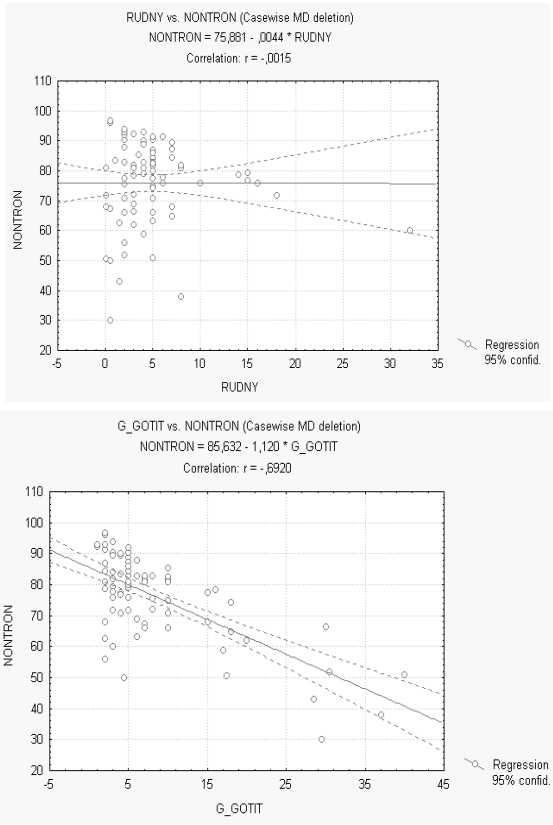


Fig. 5. Graphical representation of the correlation matrix for sample 1: top – between nontronite and the black ore mineral; bottom – between nontronite and hydrogoethite

The results of the correlation analysis for laboratory-technological sample 2 are presented in Table 6 and in Figure 6. A positive correlation is observed between the quantity of hydrogoethite and Fe_{tot} (r = 0.43); the content of quartz and nickel (r = 0.46); Fe_{tot} and cobalt (r = 0.60). Conversely, a negative correlation is established between the content of hydrobiotite and hydrogoethite (r = -0.51); the quantity of hydrogoethite and nontronite (r = -0.61); beidellite and black ore minerals (r = -0.44); Fe_{tot} and quartz (r = -0.72); nickel and cobalt (r = -0.49). No significant correlations are identified between other components in the correlation matrix presented in Table 6.

Table 6. *Correlation matrix of mineralogical and partial chemical composition of sample 2*

	Ore minerals	Hydrobiotite	Nontronite	Hydrogoethite	Quartz	Kaolinite	Fe_{tot}	Ni	Co
Ore minerals	1.00	.06	-.21	-.14	.39	-.44	-.10	.09	-.01
Hydrobiotite	.06	1.00	-.12	-.51	.24	-.25	-.42	-.04	-.36
Nontronite	-.21	-.12	1.00	-.61	-.38	.14	.20	.04	.07
Hydrogoethite	-.14	-.51	-.61	1.00	-.34	-.01	.43	-.25	.33
Quartz	.39	.24	-.38	-.34	1.00	-.14	-.72	.46	-.38
Kaolinite	-.44	-.25	.14	-.01	-.14	1.00	-.04	-.09	-.05
Fe_{tot}	-.10	-.42	.20	.43	-.72	-.04	1.00	-.23	.60
Ni	.09	-.04	.04	-.25	.46	-.09	-.23	1.00	-.49
Co	-.01	-.36	.07	.33	-.38	-.05	.60	-.49	1.00

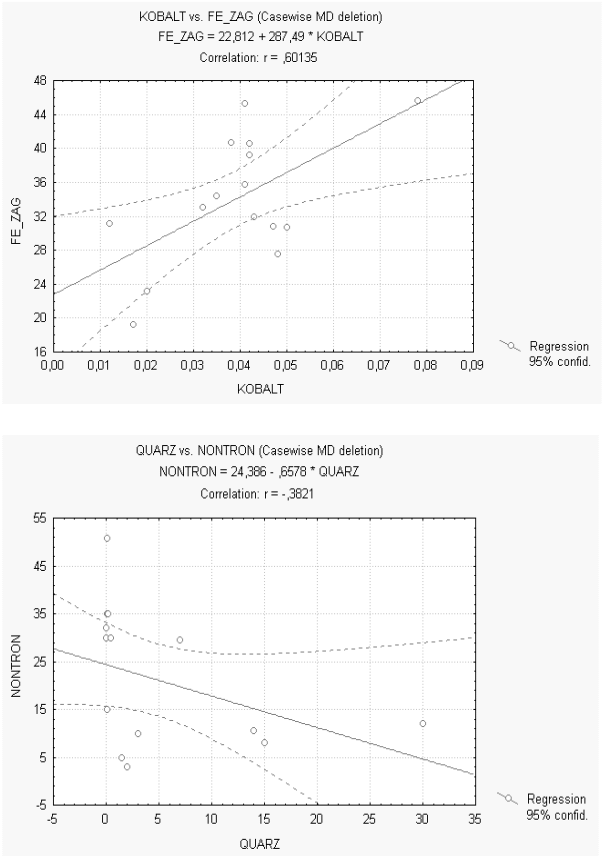


Fig. 6. Graphical representation of the correlation matrix for sample 2: top - between Fe_{tot} and cobalt; bottom - between nontronite and quartz

Mineralogical studies have determined that the primary mineral present in both the nontronite and ocherous samples is nontronite, with its quantity ranging from 14.0 to 70.0 vol.%. Secondary minerals include hydrogoethite, quartz, hydrobiotite,

chlorite, and montmorillonite, while accessory minerals consist of ilmenite, chromite, chalcopyrite, and maghemite.

An analysis of the chemical composition of nickel-containing ore reveals that the two ore samples — sample 1 (nontronite-based, silicate-nickel) and sample 2 (ochreous, iron-nickel)— are composed of the same minerals but differ in their quantitative ratios. The mass fractions of Fe_{tot} are 16.8% and 34.4% respectively for samples 1 and 2, while the SiO_2 content is 48.48% for sample 1 and 26.9% for sample 2. The quartz content measures 10.62% in sample 1 and 4.43% in sample 2.

Thermodynamic modelling

Thermodynamic calculations were performed using the ASTRA software package over a temperature range of 300–3000 K, at a pressure of 1.0 MPa, with nitrogen-oxygen (air) as the heat carrier.

For calculating the phase composition and equilibrium characteristics, a reference database containing thermodynamic, thermophysical, and thermochemical properties of individual substances is used.

The input data for calculating the composition and parameters of the equilibrium state comprise three categories:

- directives that provide specific instructions for a particular calculation variant, defining the conditions under which the calculation is executed and used to configure the programme;
- input data that define the elemental composition of the analysed thermodynamic system, specify the parameters that determine its equilibrium conditions as well as lists of individual substances, establishing the qualitative composition of condensed solutions; and
- thermodynamic properties that represent characteristics of individual substances formed under equilibrium conditions.

All additional parameters and constants required for organising the iterative process and calculating thermodynamic functions under equilibrium conditions are determined through interrelated values or are directly generated within the programme.

Condensed substances are treated as distinct phases as well as solid solutions, while the gas phase is modelled as a mixture of ideal gases. During the thermodynamic calculations, variations in the process conditions are considered.

The following components in the gas phase are evaluated: Na; NaO; $NaNO_2$; [O]; O_2; CO; CO_2; N_2; NO; NO_2; NaCl; Na_2Cl_2; Cl; Cl_2; Na_3Cl_3; $FeCl_2$; Cl; Fe; FeO_2; $FeCl_3$.

In the condensed state, the following components are analysed: Fe_2O_3; $FeO{\cdot}Fe_2O_3$ (Fe_3O_4); SiO_2; Al_2O_3; $MgSiO_3$; $MgO{\cdot}MgSiO_3$ (Mg_2SiO_4); $MgO{\cdot}Al_2O_3$ ($MgAl_2O_4$); MgO; $CaO{\cdot}N_2O_5$ (Ca_2O_6); $CaCO_3$; $CaSiO_3$; $CaSiO_3{\cdot}Ca_2SiO_4$ ($Ca_3Si_2O_7$); $NaNO_3$; Na_2SiO_3; $SiO_2{\cdot}Na_2SiO_3$ ($Na_2Si_2O_5$); Na_2CO_3; $NaFeO_2$; Ni; NiO; NaCl. During the calculations, the ore-coal ratio of and the ore-salt ratio vary from 100:1 to 100:15.

Laboratory procedures and equipment

Laboratory studies are conducted using standard testing methods for mechanical and chemical beneficiation technologies.

The primary equipment utilised includes jaw crushers, magnetic and electrical analysers, flotation machines, a stirred reactor of 0.5 to 1.5 L, vacuum filtration equipment with a Büchner funnel of 7.5 to 9.5 cm in diameter, a pH meter of the type pH-121 equipped with a glass electrode EZL-43-07 and a reference electrode (silver-chloride EZL-IMZ electrode), a muffle furnace, a shaft furnace, and a drying oven.

The mineralogical composition of the ore and the products of magnetic separation are examined using a MBS-9 binocular microscope and a Nu reflected light microscope.

Following the thermodynamic analysis of the charge materials, reducing the number of experiments, the processing of oxidised nickel ores is conducted through segregation. The following parameters are varied during the process: reduction temperature (600–1000°C), reduction duration (0.5–3 hours), coal consumption (1–10%), and consumption of the chlorinating agent NaCl (2–10%).

Upon optimisation of the process, 15 kg of raw material is roasted for research purposes to investigate the processing of nickel bearing material. These tests are conducted in three directions on both samples: a) physical-mechanical beneficiation, b) flotation beneficiation, and c) chemical beneficiation.

Prior to the studies, the ore is thoroughly quartered and homogenised using the ring-cone method. The granulometric composition of the input ore and the beneficiation products is determined with a set of sieves, featuring a scale modulus of 2, operated on a mechanical shaker.

Based on the sieve analysis of the ore, ground to 0.074 mm, dependencies of the yield of finished fractions are built as functions of the grinding time until 90% of the fraction is ready. The specific productivity q of the mill is calculated using the following formula:

$$q = (60 \times P \times 0{,}9) / (t \times V), \ \text{kg/(dm}^3\text{•hour)} \quad (1)$$

where P is the ore charge, kg; t is the grinding time required to obtain 90% of the desired class, hours; V is the mill volume, dm^3.

Productivity for the newly q' acquired class is calculated by the formula:

$$q' = q \times (\beta_2 - \beta_1) / 100, \ \text{kg/(dm}^3\text{•hour)}$$

where β_1 is the mass fraction of the minus 0.074 mm class in the input product; β_2 is the mass fraction of the minus 0.074 mm class in the ground product.

The ore is ground for laboratory tests in a laboratory ball mill (type 75A-ML). Magnetic analysis of the ore is performed using an electromagnetic roller separator (model 138T-SEM).

Wet magnetic beneficiation, aimed at isolating the strongly magnetic fraction, is conducted using a drum separator (model 237-SE).

Laboratory flotation tests are carried out on a laboratory mechanical flotation machine (model 237 FL-A) with chamber volumes varying by 0.5 dm^3. The air flow rate is maintained at 40 dm^3/m^3 of suspension, with the impeller speed set to 2500 rpm. The sample mass for the tests in an open cycle is 143 g, while in closed-cycle tests, it is 140 g. Tap water is used for the experiments.

The selection of reagents and reagent regimes is guided by standard flotation practices for nickel ores. Xanthate is utilised as a collector, while T-80 is used as a frother. Reagent consumption ranges are 0.5–1.5 kg/t for the collector and 0.05–0.3 kg/t for the frother.

Results and discussion

In this study, thermodynamic calculations are carried out for iron- and nickel-containing systems corresponding to samples 1 and 2. The optimal parameters for the reduction process are identified, and the influence of temperature and the gas phase

composition on the equilibrium state and the ratio between components is determined.

The effect of the mass fraction of coal and sodium chloride on the equilibrium composition and energy performance of the process is also assessed. The optimal sintering temperature is determined to be 1300 K (1023°C), with the ratio of the solid input concentrate to the mass fraction of salt being 100:2 for sample 1 and 100:10 for sample 2.

Thermodynamic calculations of the Ni-Fe-Si-Na-Al-Mg-Ca-C-O-N system, formed during sintering, demonstrate the feasibility of the complete transition of nickel from the oxide part of the ore to the metallic state. As shown in Table 7, an increase in temperature corresponds to an increase in specific energy consumption.

Table 7. *Dependency of specific energy consumption (kJ/kg) on the ratio (L) of input material to carbon in the specified temperature range*

T, K \ L	100:2	100:6	100:8	100:10	100:15
500	2272.93	2098.96	2130.79	2332.77	2544.43
1300	11067.42	7190.06	7552.59	7915.03	8278.92
1700	23366.28	14663.44	15134.52	15605.52	16077.05

During the technological studies conducted at the laboratories of Kryvyi Rih National University, the oxidised nickel ore intended for successful leaching in ammoniac solutions is first subjected to reduction roasting to achieve selective nickel reduction. The nickel-containing charge is subsequently analysed using thermogravimetric methods, with the results presented in Figure 7.

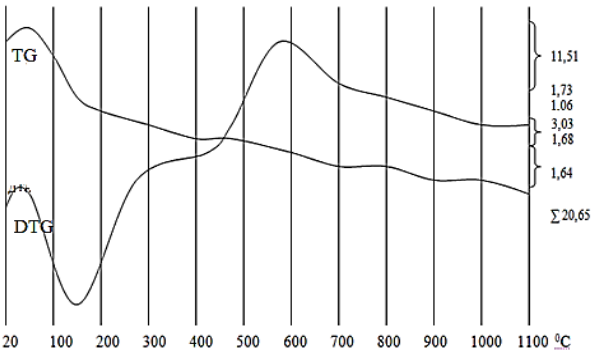


Fig. 7. Results of thermogravimetric analysis of the nickel-containing charge

The analysis of the temperature ranges reveals the following: under the temperature range of 20–150 °C, the main mass loss (~12.5%) is accompanied by a pronounced endothermic peak. This indicates the intensive removal of physically bound moisture from hydrated minerals.

Under the temperature range of 150-400 °C, further mass loss (~3%) and a deep endothermic effect are observed. This corresponds to the dehydroxylation of iron, aluminium, magnesium hydroxides or other minerals.

Under the temperature range of 400-700 °C, there is a mass loss of approximately 3.05% with smooth thermal effects. This is likely associated with continued dehydroxylation, decomposition of hydroxides, and the formation of oxide phases.

Under the temperature range of 700-1000+ °C, there are residual mass losses (~3.3%) and minor thermal effects. Structural stabilisation, crystallisation of nickel oxides, and completion of phase transitions are observed.

According to the thermogravimetric analysis, the total mass loss amounts to 22.25%, indicating a significant presence of hydrated minerals and hydroxides in the charge. The greatest loss occurs below 150 °C, suggesting a high moisture content in the charge. In the intermediate temperature range, active processes of dehydroxylation and phase transformations take place. These findings are used to optimise thermal conditions for pre-roasting or reduction. At the same time, transitional forms of Fe, Ni, and Al oxides should be considered during subsequent technological operations.

The charge prepared for reduction is pre-dried to a moisture content of 3% and ground to a particle size of -0.16 mm (98%). It should be noted that this level of grinding represents the limit, as further reduction in particle size results in a loss of floatability.

Reduction roasting produces materials with the nickel content ranging from 2.02% to 3.03%. To enhance the economic efficiency of leaching, the use of beneficiated products is essential. Accordingly, after the reduction roasting of the nontronite sample, the roasted materials are ground to -0.074 mm and subjected to separation using a magnetic analyser with a magnetic field strength of 80–800 kA/m. The analysis indicates that the optimal magnetic field strength is 80 kA/m, yielding a nickel recovery of 85.99% into the concentrate (non-magnetic product) for sample 1, and 83,33 % - for sample 2 with the nickel content of 3.2% in the non-magnetic fraction for sample 1 and 2.5 % - for sample 2. The results of the mineralogical analysis (Table 8) demonstrate that after magnetic separation, the nickel-containing component (grey clay mineral) primarily accumulates in the non-magnetic fraction (Figures 8, 9), with a portion also present in the magnetic product.

Table 8. *Results of the study of the composition of magnetic separation products*

Components	Magnetic fraction	Non-magnetic fraction
Bronze kinglet	0.5	0.4
Magnetite	34.3	5.3
Hematite	8.9	17.2
Dispersed hematite	9.6	12.3
Maghemite	4.9	0.7
Quartz	14.3	16.7
Mica	2.5	4.3
Grey clay mineral	22.4	40.9
Salt	2.2	0.0
Coal	0.4	2.2
Total	100.0	100.0

Quartz and mica exhibit similar behaviour. A higher degree of magnetic separation could potentially be achieved through further grinding of the input material.

The mass fraction of nickel in the non-magnetic product is 2.5-3.2%, while the mass fraction of nickel in the magnetic product is 1.79-1.82%. This indicates a low selectivity of separation during the magnetic separation of the roasted ore,

due to the dispersed nature of nickel distribution within the minerals.

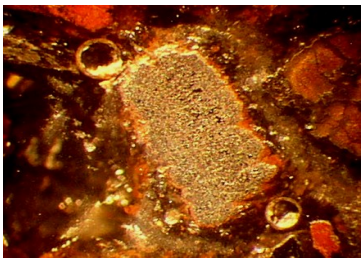


Fig. 8. Hematite fragment (grey) with a dispersed hematite rim (orange); non-magnetic product. Binocular observation (MBS-9). Magnification 30X

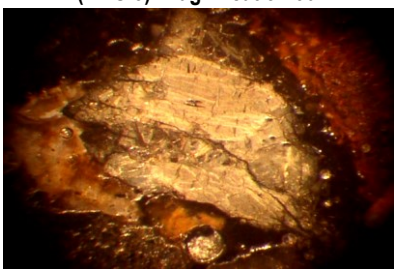


Fig. 9. Fragment of grey clayey mineral; non-magnetic product. Binocular observation (MBS-9). Magnification 30X.

Given the high nickel content in the magnetic product, attributable to the dispersed nature of nickel distribution within the minerals, the product is subjected to flotation. This process reduces the nickel content from 1.79% to 1.59%.

For the flotation studies of the roasted product, the cooled material is ground to achieve 80–90% of the -0.074 mm fraction. The pulp, with a solid-to-liquid ratio (S:L) of 1:1, is heated to 700°C and agitated for 30 minutes with copper sulphate (3 kg/t). Subsequently, 900 g/t of butyl xanthate and 100 g/t of frother are added, and nickel flotation is conducted. Flotation concentrates are obtained containing 3-5% nickel with a yield ranging from 17% to 50% from sample 1. From sample 2, flotation concentrates are obtained containing 3-4% nickel with a yield of 7.4-46%. Magnetic cleaning of the rough flotation concentrate in a field with a strength of 80 kA/m allows for an increase in the nickel content in the concentrate: up to 8% for from sample 1, up to 7% for sample 2.

The roasted product was also subjected to leaching. Ammoniac leaching is performed by varying the parameters S:L from 1:7 to 1:10, with the mass fraction of ammonium salts ranging from 100 to 150 g/dm³. The data indicate that the highest nickel recovery (88%) occurs for the materials reduced at a temperature of 900°C.

The results of studying the effect of reduction time on nickel recovery into the solution (Figure 10) show that the optimal reduction time is 2 hours. Extending the reduction time beyond this has minimal impact on improving subsequent nickel leaching. During the leaching of reduced nickel matte, intensive aeration of the pulp is observed to be essential, as the dissolution of nickel in ammonia solutions occurs with the release of hydrogen. In this process, nickel is solubilized as divalent ion. Ammonia sublimation is further conducted at a temperature of 80–90°C, resulting in the formation of hydrated nickel oxide. Studies indicate that in the presence of an excess of NH_3 (2–3%) in the solution, nickel carbonate is formed. Following thickening and filtration, a precipitate with a moisture content of 65–70% is obtained. After drying in a drying oven, the final product contains 47% Ni, 0.5% Co, and 0.8% Fe.

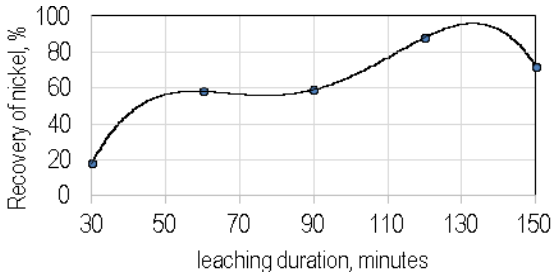


Fig. 10. Dependency of nickel recovery into the ammonia-carbonate solution on the duration of reduction (t = 1023°C, S:L= 1:1)

Thermogravimetric analysis of nickel carbonate reveals mass loss and thermal effects across the temperature range of 20 to 1100 °C. The analysis of temperature intervals shows the following. Within the range of 20–150 °C, a mass loss of approximately 0.9% and a moderate endothermic peak are observed. This corresponds to the removal of physically bound and crystallization water from the nickel salt. Within the range of 150–450 °C, a mass loss of approximately 8.04% occurs, accompanied by a series of endothermic peaks. This indicates dehydroxylation processes ($Ni(OH)_2 \rightarrow NiO + H_2O$), possibly linked to the decomposition of main impurity salts. Within the range of 450–750 °C, a 19.3% mass loss and a pronounced endothermic effect were observed. This is the primary decarbonisation zone ($NiCO_3 \rightarrow NiO + CO_2$). Within the range of 750–900 °C, a mass loss of 17.44% with a clear endothermic peak is noted. This signifies the complete decomposition of residual carbonates and the formation of stable nickel oxide (NiO).

In total, the overall mass loss is 45.69%, which corresponds to the complete dehydration and decarbonisation of the sample. The main processes involved are water removal (up to 150 °C), dehydroxylation (150–450 °C), and $NiCO_3$ decomposition (450–900 °C).

The final product is stable nickel oxide (NiO), formed as a result of the thermal decomposition of the carbonate. This data is crucial for selecting the optimal roasting temperature mode for nickel oxide production.

This process yields a product with the following content of metals: 70% Ni, 0.6–0.9% Co and 0.8–1.0% Fe.

Physicochemical studies of the obtained product reveal that it primarily consists of a mixture of nickel oxides. Furthermore, the dependency of the specific filtration productivity (Figure 11) of the roasted and leached product on the roasting temperature is examined.

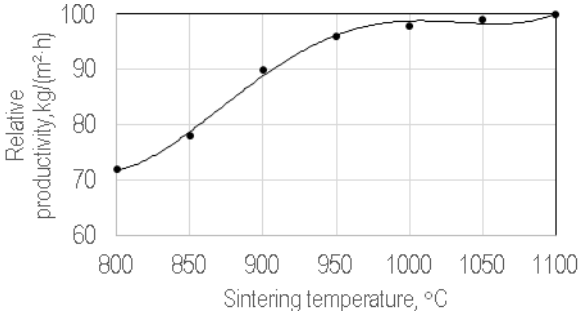


Fig. 11. Dependency of the relative filtration productivity of the leached sintered product on the roasting temperature

The suspension sent for dewatering has a solid phase with a large specific surface area, which complicates filtration. To intensify this process, a series of dewatering experiments is conducted using the flocculant polyacrylamide (PAA). The influence of factors such as the dose of the flocculant and its mass concentration is studied. Process efficiency is evaluated based on filtration productivity and filtrate purity. Experimental results determine that the optimal PAA consumption is approximately 300 g/t of solid material. Under these conditions, the specific filtration productivity reaches its maximum value of 30 kg/m²·per hour.

The results of laboratory studies for the first time facilitate the development of a flowsheet for obtaining nickel-containing products (Figure 12).

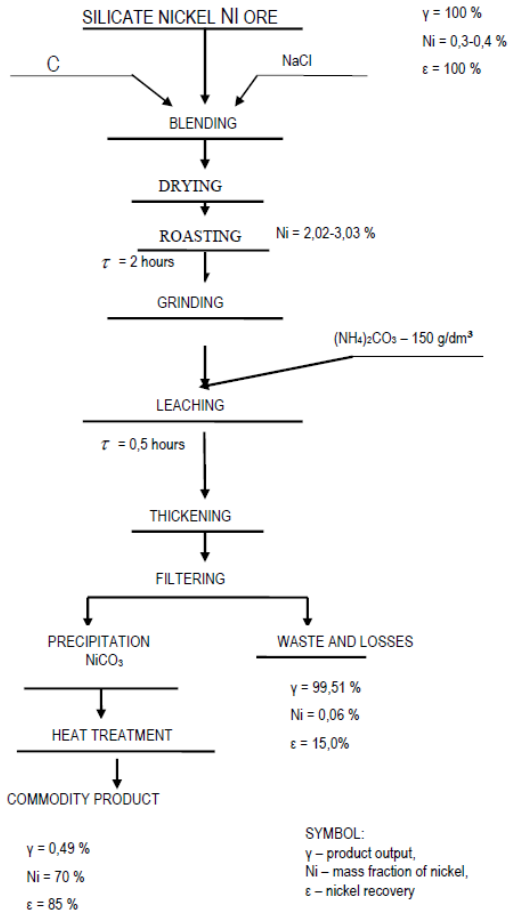


Fig. 12. Flowsheet for the production of a commodity nickel product from Ukrainian silicate ore

The following main stages can be highlighted:

- Oxidised nickel ores are mixed with a reducing agent (coal, 10% of the initial ore) and sodium chloride (approximately 5%). The charge is homogenised, dried at 100°C, and subjected to roasting (t = 1000°C, τ= 2 hours).
- The roasted product, after disintegration to a particle size of -0.16 mm, is directed to ammoniac leaching (ammonium salt concentration of 100–150 g/dm³, t = 25°C, τ = 0.5 hours) under intensive aeration, followed by thickening and filtering. The filtered leaching tailings, after neutralisation, can be utilised as a construction material.
- Ammonia is removed from the leaching solutions by heating (t = 80°C, τ = 1 hour) and is subsequently recycled into the leaching of the roasted product, resulting in the precipitation of pure nickel carbonate.
- The chemical nickel carbonate, after filtration and washing on press filters (specific filtration load: 175–200 kg/m²·hour), is directed to thermal treatment.

Conclusions

With the advancement of the new energy industry, nickel, has been recognised as a strategic mineral by numerous countries and is garnering increasing global attention. The present paper explores the progress of research on the extraction of nickel from lateritic silicate ores of Zakhidno-Lashchivka area through hydrometallurgical processes. The primary findings are as follows:

1. Based on the analysis of the mineral composition of standard samples and the results of the chemical analysis, the laboratory-technological sample is classified into two types according to the content of slag-forming components: (1) nontronitic (sample 1) and (2) ochreous (sample 2). Both samples predominantly consist of the same minerals but vary in their quantitative proportions. This distinction is also evident in their chemical composition, with Fe_{tot} content being 34.4% and 16.8%, and SiO_2 content being 26.9% and 48.48% for samples 2 and 1, respectively.

2. The principal mineral in the silicate-nickel ore is nontronite, with its content ranging from 4.0 to 70.0 vol.%. The ochreous variety is predominantly composed of hydrogoethite and goethite. These minerals are present as free fragments and aggregates, often in association with nontronite, quartz, and black ore minerals such as maghemite, chromite, and ilmenite.

3. To achieve effective leaching of oxidised nickel ore in ammoniac solutions, the ore should undergo reduction roasting as a preliminary step, facilitating selective nickel reduction. This process yields products with a nickel content ranging from 2.02% to 3.03%.

4. The results of magnetic and flotation beneficiation of nickel ore after reduction roasting demonstrate low selectivity. The nickel content in concentrates obtained by magnetic separation is 2.5–3.2% (in the non-magnetic fraction) while it is 1.79-1.82% in the magnetic fraction. Flotation of the roasted product yields concentrates containing 3–5% nickel. Magnetic re-cleaning of the rough flotation concentrate in a field of 80 kA/m allows an increase in nickel content in the concentrate obtained from sample 1 to 8%, and from sample 2 to 7%.

5. The optimal treatment process is identified as chemical leaching of the raw material and ammonia sublimation at a temperature of 800–900 °C. As a result of sublimation, nickel carbonate is obtained. After thickening and filtration, a precipitate with a moisture content of 65–70% is produced, which, after drying in a drying oven, contains 47% Ni, 0.5% Co, and 0.8% Fe.

6. The findings from laboratory investigations for the first time facilitate the development of a flowsheet for chemical beneficiation of silicate ores found in Ukraine. This flowsheet demonstrates that an ore with a nickel content of 0.3-0.4% can produce a commodity product with 70% Ni, 0.6-0.9% Co, and 0.8-1.0% Fe**,** following a process of sequential roasting, ammoniac leaching, and nickel carbonate roasting**.** Nickel recovery to the final product is 85%.

References

Andersson, P., (2020). Chinese assessments of “critical” and “strategic” raw materials: Concepts, categories, policies, and implications. *The Extractive Industries and Society*, *7* (1), 127-137. https://doi.org/10.1016/j.exis.2020.01.008

Babii, K.V., Bubnova, O.A., Maleiev, Y.V., Riumina, D.M., Levchenko, K.S. & Ikol, O.O. (2024). *Resursy stratehichnykh korysnykh kopalyn Ukrainy: monohrafiia.* PBP ‘Ekonomika’ - Dnipro (in Russian). https://www.researchgate.net/publication/390199010

Boroumand, Z., Abdollahi, H., Pashaki, S.N.A., Mirsaleh Mirmohammadi, & Ghorbani, Y. (2025). Enhanced oxidative bioleaching for nickel and metal recovery from arsenic ores moves toward efficient and sustainable extraction. *Chemosphere, 370,* Article 143944 https://doi.org/10.1016/j.chemosphere.2024.143944

Brown, T. (2018). Measurement of mineral supply diversity and its importance in assessing risk and criticality. *Resources Policy, 58*, 202-218. doi: 10.1016/j.resourpol.2018.05.007

Carpen, H.L. & Giese, E.C. (2022). Enhancement of nickel laterite ore bioleaching by Burkholderia sp. using a factorial design. *Applied Water Science, 12* Article 181 doi: 10.1007/s13201-022-01704-5

Chaerun, S.K., Sulistyo, R.S., Minwal, W.P. & Mubarok, M.Z. (2017). Indirect bioleaching of low-grade nickel limonite and saprolite ores using fungal metabolic organic acids generated by Aspergillus Niger. *Hydrometallurgy, 174*, 29-37. doi: 10.1016/j.hydromet.2017.08.006

Chaerun, S.K., Winarko, R. & Yushandiana, F. (2023). Biohydrometallurgy: Paving the way for a greener future of mineral processing in Indonesia. *Current Research on Biosciences and Biotechnology, 5*(1), 299-307. doi: 10.5614/crbb.2023.5.1/8kiz3aoe

Fan, Q., Yuan, S. Wen, J., & He J. (2024). Review on comprehensive utilization of nickel laterite ore. *Minerals Engineering, 218,* Article 109044 https://doi.org/10.1016/j.mineng.2024.109044

Li, J.H., Li, Y.Y., Zheng, S., Xiong, D.L., Chen, H. & Zhang, Y.F. (2015). Research review of laterite nickel ore metallurgy. *Nonferrous Metals Science and Engineering, 6* (1), 35-40 (in Chinese with English abstract). doi: 10.13264/j.cnki.ysjskx.2015.01.007

Li, J.H., Xu, Z.F. & Wang, R.X. (2019). *Fundamental research on chlorination metallurgy technology for lateritic nickel ores*. Metallurgical Industry Press, Beijing.

Nurjaman, F., Bahfie, F., Herlina, U., Astuti, W. & Suharno, B. (2020). Kajian literatur parameter proses reduksi selektif bijih nikel laterit. *Metal Indonesia, 42*(2), 63. doi: 10.32423/jmi.2020.v42.63-71

Pandey, N., Tripathy, S.K., Patra, S.K. & Jha, G. (2023). Recent progress in hydrometallurgical processing of nickel lateritic ore. *Transactions of the Indian Institute of Metals, 76*(1), 11-30. doi: 10.1007/s12666-022-02706-2

Roberto, F. & Schippers, A. (2022) Progress in bioleaching: part B, applications of microbial processes by the minerals industries. *Applied Microbiology and Biotechnology, 106*(18), 5913–5928. doi: 10.1007/s00253-022-12085-9

Santos, A.L., Dybowska, A., Schofield, P.F., Herrington, R.J. & Johnson, D.B. (2020). Sulphur-enhanced reductive bioprocessing of cobalt-bearing materials for base metals recovery. *Hydrometallurgy, 195,* Article 105396. doi: 10.1016/j.hydromet.2020.105396

Smailov, K. M., Nuruly, Y. & Beisenbiyeva, U. Z. (2022). Development of an Innovative Technology for the Complex Extraction of Nickel and Cobalt from Iron-Silicate Ores. *European Journal of Advanced Chemistry Research, 3*(4), 10-15. https://doi.org/10.24018/ejchem.2022.3.4.123

Tian, Q.H., Li, Z.C., Wang, Q.M., Wang, S.S. & Guo, X.Y. (2023). Present situation of laterite nickel ore resources and research progress of smelting technology. *The Chinese Journal of Nonferrous Metals, 33*(9), 2975-2997 (. doi: 10.11817/j.ysxb.1004.0609.2022-43438

Wani, O.B., Khan, S., Shoaib, M., Gonçalves, C., Chen, Z., Zeng, H. & Bobicki, E.R. (2024). Processing of low-grade ultramafic nickel ores: A critical review. *Minerals Engineering, 218,* Article 108976. https://doi.org/10.1016/j.mineng.2024.108976

Yue, L., Zhouliang, T., Yuming, L., Changlong, L., Peipei, H. & Jingyi, L. (2024). Past, present and future of high-nickel materials. *Nano Energy, 119,* 2211-2855. https://doi.org/10.1016/j.nanoen.2023.109070

Zappala, R., Donald, M. & Pownceby, M.I. (2023). Nickel laterite beneficiation and potential for upgrading using high-temperature methods: A review. *Mineral Processing and Extractive Metallurgy Review, 45*(7), 267-289. doi: 10.1080/08827508.2023.2265533

Zhang, Z-f, Zhang, W-b, Zhang, Z-g & Chen, X-f (2025). Nickel extraction from nickel laterites: Processes, resources, environment and cost. *China Geology, 8*(1),187-213. https://doi.org/10.31035/cg2024124